Forward and Backward Beam-Scanning Tri-Band Leaky-Wave Antenna

Debabrata K. Karmokar, *Member, IEEE*, Yingjie Jay Guo, *Fellow, IEEE*, Pei-Yuan Qin, *Member, IEEE*, Karu P. Esselle, *Fellow, IEEE*, and Trevor S. Bird, *Life Fellow, IEEE*

***Abstract*—The main limitations of uniform half-width microstrip leaky-wave antennas (HW-MLWAs), namely a single operating band and only forward beam scanning, are overcome here with an HW-MLWA loaded with periodic L-shaped slots. The antenna exhibits tri-band operation, and the main beam can be steered in the forward direction in one band, and in the backward direction in the other two bands. Its size is halved with a shorting wall. The antenna was fabricated and tested to validate the concept, and the measured and simulated results agree very well. The measured matched (10-dB return loss) bandwidths of the prototype are 22.34% (5.05–6.32 GHz), 15.85% (8.77–10.28 GHz), and 11.21% (12.63–14.13 GHz) in the first, second, and third bands, respectively. The beam-scanning ranges of the prototyped antenna are 30° to 64°, −75° to −18°, and −19° to −4° when the frequency sweeps from 5 to 6 GHz, 8.85 to 10.5 GHz, and 13 to 14.25 GHz, respectively. The measured peak gains (within the scanning range) are 12.4, 14.3, and 14.7 dBi in the first, second, and third bands with variations of 2.5, 3.4, and 3.1 dB, respectively.**

***Index Terms*—Beam scanning, half-width (HW), higher order mode, leaky-wave antenna (LWA), L-slot, microstrip, tri-band.**

I. Introduction

MICROSTRIP leaky-wave antennas (MLWAs) are attractive due to their inherent beam-scanning capabilities from planar low-profile structures. The inherent beam scanning of leaky-wave antennas (LWAs) makes them suitable for various applications such as multipoint communications and automotive radar [1]–[5]. Microstrip-based LWAs were proposed in 1978 [6] with methods to excite a higher order microstrip mode. Later on, microstrip-based LWAs and the radiation properties of higher order microstrip modes were explained in more detail in [7] and [8].

Manuscript received January 12, 2017; accepted March 4, 2017. Date of publication March 21, 2017; date of current version July 17, 2017. This work was supported by the Australian Research Council under a Discovery Project under Grant 160102219.

D. K. Karmokar, Y. J. Guo, and P.-Y. Qin are with the Global Big Data Technologies Centre, Faculty of Engineering and Information Technology, University of Technology Sydney, Ultimo, NSW 2007, Australia (e-mail: dkkarmokar@ieee.org; jay.guo@uts.edu.au; Peiyuan.Qin@uts.edu.au).

K. P. Esselle is with the School of Engineering, Faculty of Science and Engineering, Macquarie University, Sydney, NSW 2109, Australia (e-mail: karu@ieee.org).

T. S. Bird is with the Global Big Data Technologies Centre, Faculty of Engineering and Information Technology, University of Technology Sydney, Ultimo, NSW 2007, Australia, and also with the School of Engineering, Faculty of Science and Engineering, Macquarie University, Sydney, NSW 2109, Australia (e-mail: ts.bird@ieee.org).

Color versions of one or more of the figures in this letter are available online at http://ieeexplore.ieee.org.

Digital Object Identifier 10.1109/LAWP.2017.2685439

The direction of the main beam of an LWA is given by the usual expression for leaky modes, i.e.,

$$\theta(f) = \sin^{-1}\left[\frac{\beta(f)}{k_0(f)}\right] \tag{1}$$

where θ is the angle between the main beam and the broadside direction, k_0 is the free-space wavenumber, and β is the phase constant [3]. With a change of frequency the value of β/k_0 changes, which in turn changes the beam direction [9].

Owing to their simple structure and potential applications, LWAs have gained rigorous research interest, and the field is developing with new antenna designs to overcome different limitations. In order to enable a microstrip line to radiate, higher order modes of the microstrip line need to be excited [10]. A half-width (HW) MLWA (HW-MLWA) proposed in [11] presents an easy method to achieve radiation from the first higher order mode of a microstrip line without using any special feed mechanism. Because of the structural simplicity, a large amount of research has been conducted on HW-MLWAs. However, most of the HW-MLWAs operate in a single frequency band. Some LWAs offer dual-band operation, including a periodic composite right/left-handed (CRLH) LWA [12], a substrate integrated waveguide (SIW)-based CRLH LWA [13], and periodic HW-MLWAs [3]. Though the periodic HW-MLWAs in [3] can scan beam in two bands, in the forward and backward directions, the upper beam-scanning limit in the backward direction is lower than the forward direction.

The research on achieving tri-band operation from an LWA is very limited. An LWA based on a CRLH SIW structure with three operating bands has been proposed in [14]. The antenna offers two CRLH bands, one in lower frequencies and another at higher frequencies, and a right-handed band in between. To the authors' best knowledge, there is no tri-band LWA demonstrated based on an HW-MLWA structure.

In this letter, a periodic HW-MLWA is proposed, which operates in three different bands, and the antenna beam can be steered in the forward direction in one band and the backward direction in the other two bands. Unlike SIW-based LWAs, the proposed antenna requires only half of the microstrip width and hence halves the size of the antenna. To achieve this, the structure requires only one shorting wall (via array). To achieve tri-band operation a new unit cell was designed using an L-shaped slot in each unit cell. To verify the concept, the antenna has been prototyped and is printed on a single-layer substrate.

II. Unit Cell Design Using Dispersion Analysis

The properties of an LWA can be estimated initially by analyzing the dispersion characteristics of a unit cell.

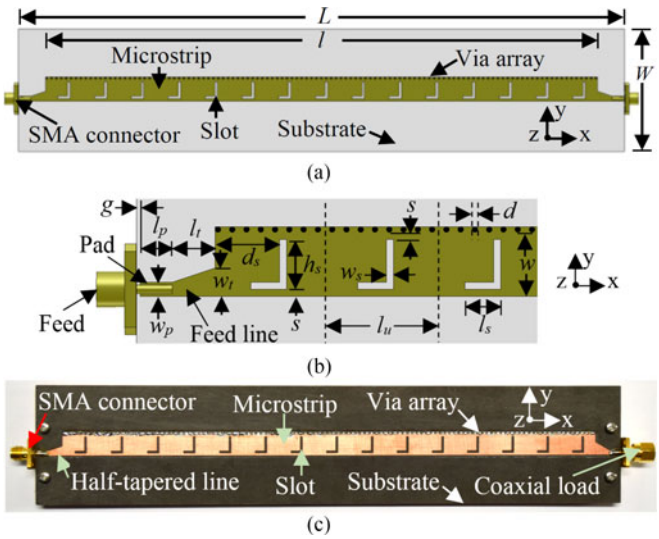

Fig. 1. L-slot-loaded tri-band HW-MLWA. (a) Complete structure (top view), (b) unit cell and feed section, and (c) fabricated prototype (top view).

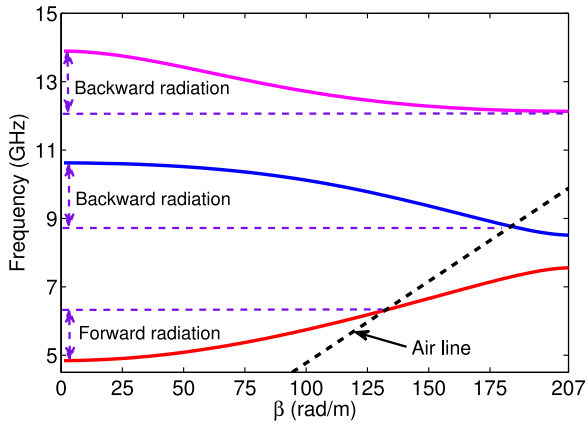

Fig. 2. Dispersion diagram of an L-slot-loaded HW-MLWA unit cell.

The eigenmode solver of CST Microwave Studio [15] was used to obtain the dispersion diagram of a unit cell. Different types of HW-MLWA unit cells were investigated for multiband operation. It was found that an L-slot-loaded unit cell provides three radiation bands with the possibility of leaky-mode radiation in each one. All that is needed is a suitable guiding structure to excites these modes. The length of the unit cell is smaller than the unit cells used in [3]. The antenna is designed using 15 L-slot-loaded unit cells. Fig. 1 shows the configuration of the antenna and Fig. 1(b) shows the top view of the unit cell. All the dimensions of the unit cell are given in Section III.

The dispersion diagram of the L-slot-loaded unit cell is shown in Fig. 2. The heavy dotted line in Fig. 2 corresponds to an air line where $\beta/k_0 = 1$. The dispersion diagram shows that there are three radiation regions in three frequency bands. In the first band, the unit cell has right-handed properties (forward radiation), and in the other two bands (second and third), the structure exhibits left-handed properties (backward radiation). On the other hand, uniform HW-MLWAs operate in a single band and radiation occurs in the forward direction [3]. The dispersion diagram also shows that β/ω changes as the frequency varies and hence the direction of the main beam. The direction of the main beam (θ) of a long LWA (ideally infinite length) can be determined from the dispersion diagram using (1).

III. Configuration of the Antenna

Fig. 1(a)–(c) illustrates the typical top view, unit cell and matching section, and the fabricated prototype (top view), respectively.

CST Microwave Studio was used to design the antenna and for optimization of its parameters. The prototype is printed on a 1.575-mm-thick (i.e., $t = 1.575$ mm) Rogers RT/duroid 5880 substrate (dielectric constant = 2.2 and loss tangent = 0.0009). The dimensions of the substrate and the ground plane of the complete antenna are 247 × 50 mm^2 ($L \times W$) and the dimensions of the microstrip line are 225 × 9 mm^2 ($l \times w$). In terms of the free-space wavelength (λ_0), the length (L) of the substrate and the length (l) of the microstrip are 4.53λ_0 and 4.125λ_0, respectively, where the value of λ_0 is calculated at 5.5 GHz. An L-shaped slot [see Fig. 1(b)] is used at the middle of the microstrip line, and the dimensions of the slot have been optimized through parametric studies with CST to obtain tri-band operation with the best impedance matching in the three operating bands. The dimensions of a slot are height (h_s) = 7 mm, length (l_s) = 5 mm, and width (w_s) = 1 mm. The spacing (s) between the slot and the free microstrip edge or the via array is 1 mm. The distance (d_s) of the first slot from the leftmost side of the microstrip [see Fig. 1(b)] is 9 mm, and the distance between two successive slots is 15 mm (length of a unit cell, $l_u = 15$ mm). A total of 113 vias are used to short one edge of the microstrip (upper edge shown in Fig. 1) to the ground plane.

There is a matching pad at the far-left-hand side of the substrate [see Fig. 1(b)] that is connected to an SMA inner conductor, in the same plane as the microstrip, leaving a gap (g) of 0.5 mm from the substrate edge. The dimensions of the pad are 4.5 × 2 mm^2 ($l_p \times w_p$). Since the antenna is easily fed using microstrip, we conducted investigations on different types of microstrip feeds. It was found that a half-tapered line provides the best input impedance match over the band. The half-tapered matching line [see the feed line in Fig. 1(b)] is used at the left end of the microstrip between the microstrip and the pad. The dimensions of the half-tapered feed line are length (l_t) = 6 mm, width (w_t) at the microstrip end = 4 mm, and the width at the pad end is the same as the width (w_p) of the pad. A similar pad and half-tapered line are at the right-hand side of the substrate to terminate the microstrip in a 50 Ω matched load using another SMA connector.

IV. Measured and Simulated Results

A. S-Parameters

The measured and simulated S-parameters of the periodic L-slot-loaded HW-MLWA are shown in Fig. 3. It can be seen that there is excellent agreement between the simulated and the measured values. There are minor variations, and these are mostly likely due to small fabrication errors. The measured reflection coefficient remains below the −10-dB level from 5.05 to 6.32 GHz (22.34% bandwidth), 8.77 to 10.28 GHz (15.85% bandwidth), and 12.63 to 14.13 GHz (11.21% bandwidth). At 5 GHz, the reflection coefficient is −8.6 dB. Beyond 10.28 GHz, the reflection coefficient is >-10 dB, but it remains ≤ -6.4 dB up to 10.5 GHz. From 14.13 to 14.25 GHz, the reflection coefficient is >-10 dB, but remains ≤ -6 dB.

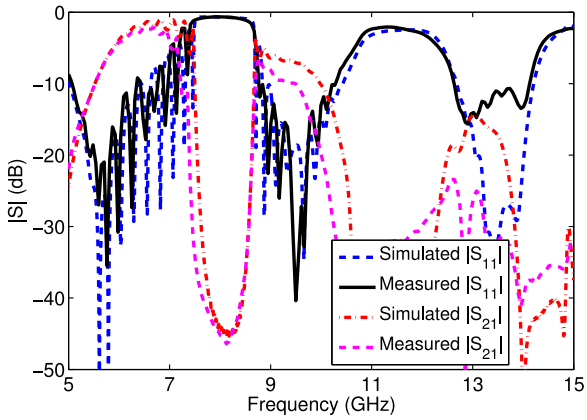

Fig. 3. Measured and simulated S-parameters of the proposed LWA.

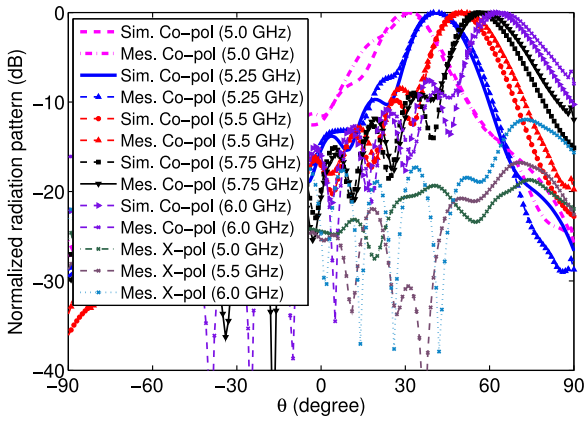

Fig. 4. Measured and simulated radiation (gain) patterns (xz-plane) of the proposed LWA in the first band.

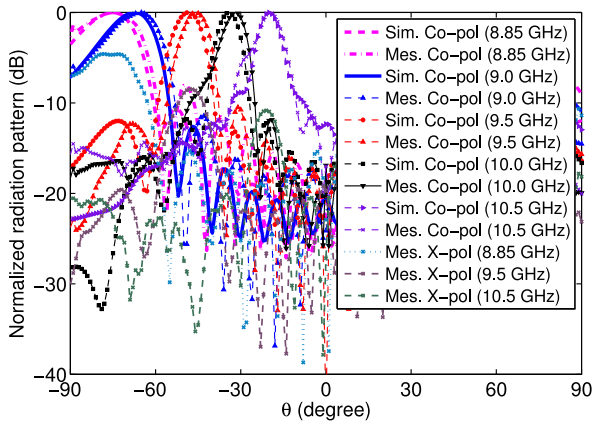

Fig. 5. Measured and simulated radiation (gain) patterns (xz-plane) of the proposed LWA in the second band.

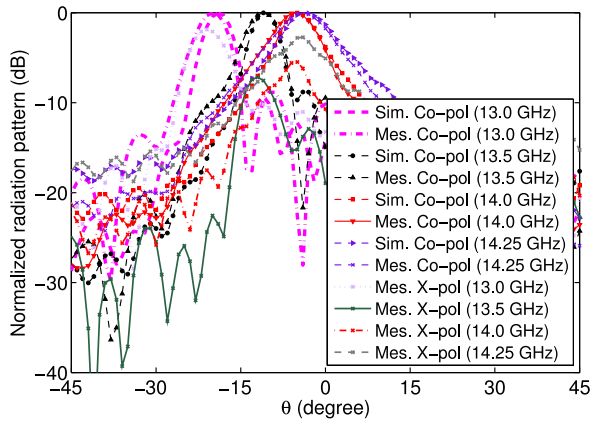

Fig. 6. Measured and simulated radiation (gain) patterns (xz-plane) of the proposed LWA in the third band.

For the first band, the transmission ($|S_{21}|$) is very low at low frequencies. For example, the measured transmission at 5 GHz is -22 dB. A simultaneous high return loss and low transmission indicate that the power is accepted by the antenna structure, but it radiates before reaching the other port [a 50-Ω coaxial load termination in Fig. 1(c)]. The transmission in the first band increases with increasing frequency (see Fig. 3). For example, the measured transmission at 6 GHz is -4.1 dB, illustrating a small amount of power remaining at the termination because of the finite length (total length of 15 unit cells) of the antenna. For the second band, the transmission is high at lower frequencies (-7.6 dB at 8.85 GHz) and reduces with frequency (-37.9 dB at 10.5 GHz), indicating good radiation at the higher frequencies in the second band. In the third band, the measured transmission remains below -23.4 dB throughout the band.

B. Radiation Patterns

The radiation characteristics of the L-slot-loaded HW-MLWA prototype were measured using the NSI700S-50 spherical near-field range at the Australian Antenna Measurement Facility. The measured and simulated xz-plane radiation patterns of the fabricated antenna in the first band are shown in Fig. 4. In the legend, "Sim." denotes simulated results (from full-wave simulation), while "Mes." indicates measurement. It can be seen that the measured results agree very well with the simulated results. From Fig. 4, it is evident that in the first band the beam points in the forward direction. At 5 GHz, the main beam is directed at 30°, which is close to the broadside direction [i.e., the $+z$-direction in Fig. 1(c)]. With an increase of frequency, the beam scans toward the endfire [the $+x$-direction is the endfire, as shown in Fig. 1(c)]. For example, at 5.5 and 6 GHz, the measured main beam directions are 50° and 64°, respectively.

The measured radiation patterns in the second and third bands are shown in Figs. 5 and 6, respectively, together with the simulated patterns. In these two bands, the beam stays in the backward direction, i.e., the θ values of the main beam are negative. In the second band, the antenna scans from near backfire [backward endfire, i.e., the $-x$-direction in Fig. 1(c)] toward the broadside direction when the frequency sweeps from low to high. In this band, the main beam scans from $-75°$ to $-18°$ (measured) when the frequency is swept from 8.85 to 10.5 GHz. In the third operating band, the main beam scans between $-19°$ and $-4°$ when the frequency is swept over the 13–14.25 GHz range. In the first band, cross polarization is low at lower frequencies and increases with the increase in frequency. In the second band, cross polarization is high at low frequencies but decreases significantly as frequency increases. In the third band, cross polarization is low around the center frequency.

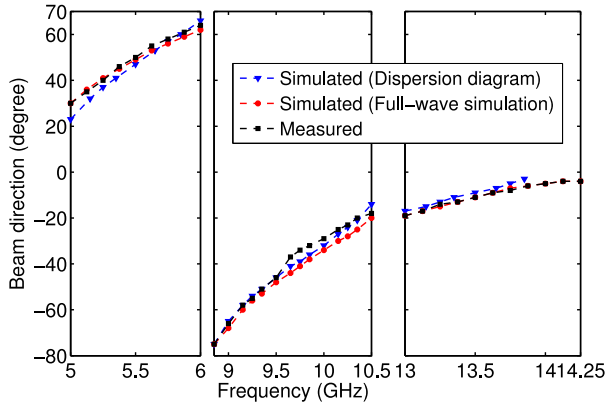

Fig. 7. Beam direction (simulated, measured, and calculated from the dispersion diagram) of the proposed LWA with frequency.

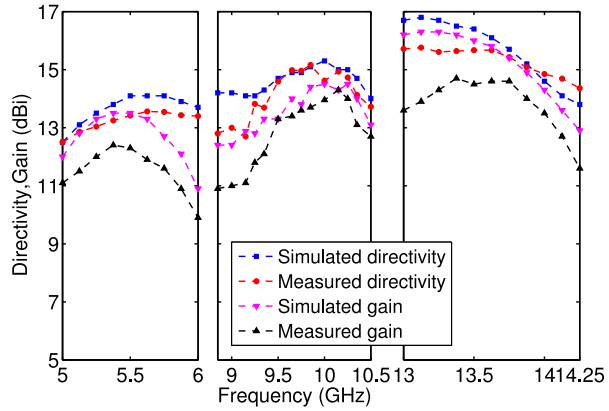

Fig. 8. Measured and simulated gain and directivity of the proposed LWA in the three operating bands.

Fig. 7 shows the beam directions (simulated, measured, and calculated from the dispersion diagram) at different frequencies in all three bands. It can be seen that there is excellent agreement between the simulated angles from the full-wave simulation and measurement. There is some difference between the calculated angle from the dispersion diagram and the measurement, because the dispersion diagram is for an infinitely long periodic structure.

C. Measured and Simulated Directivity and Gain

The measured and simulated gain and directivity of the fabricated antenna are shown in Fig. 8 for the three bands, namely 5–6, 8.85–10.5, and 13–14.25 GHz. A gain-comparison method was used for gain measurement. In the first band (see the left rectangle of Fig. 8), the peak measured gain is 12.4 dBi with a variation of gain between 5 and 6 GHz that is only 2.5 dB. In the second band (middle rectangle of Fig. 8), the measured maximum gain is 14.3 dBi with 3.4 dB variation. The peak gain (measured) in the third band (see the right plot of Fig. 8) is 14.7 dBi, and the variation is 3.1 dB. The 3-dB gain-bandwidths are more than 1, 1.25, and 1.15 GHz in the first, second, and third bands, respectively. At 5 and 6 GHz, the measured directivities are 12.5 and 13.4 dBi, respectively. In the second and third bands, the maximum measured directivities are 15.2 and 15.76 dBi, respectively.

V. Conclusion

A uniform HW-MLWA generally scans its beam only in the forward direction and in a single frequency band. A compact L-slot-loaded periodic HW-MLWA is proposed to achieve tri-band operation, and the antenna can scan the beam in the forward direction in the first band and in the backward direction in the other two bands. This new tri-band HW-MLWA is a potential candidate for many applications where beam scanning is required from a simple planar antenna structure, such as frequency-scanning radars.

The impedance bandwidths of the prototype are 1.27, 1.51, and 1.5 GHz in the first, second, and third bands, and the measured beam-scanning ranges of the prototype are 34°, 57°, and 15°, respectively. The measured peak gains of the antenna in the first, second, and third bands are 12.4, 14.3, and 14.7 dBi, and the 3-dB gain-bandwidths are greater than 1, 1.25, and 1.15 GHz, respectively. Further improvements of gain and directivity are possible by simply adding more unit cells to the design.

References

[1] T.-L. Chen, Y.-D. Lin, and J.-W. Sheen, "Microstrip-fed microstrip second higher order leaky-mode antenna," *IEEE Trans. Antennas Propag.*, vol. 49, no. 6, pp. 855–857, Jun. 2001.

[2] D. R. Jackson, C. Caloz, and T. Itoh, "Leaky-wave antennas," *Proc. IEEE*, vol. 100, no. 7, pp. 2194–2206, Jul. 2012.

[3] D. K. Karmokar and K. P. Esselle, "Periodic U-slot-loaded dual-band half-width microstrip leaky-wave antennas for forward and backward beam scanning," *IEEE Trans. Antennas Propag.*, vol. 63, no. 12, pp. 5372–5381, Dec. 2015.

[4] M. Garcia-Vigueras, J. L. Gomez-Tornero, G. Goussetis, A. R. Weily, and Y. J. Guo, "Enhancing frequency-scanning response of leaky-wave antennas using high-impedance surfaces," *IEEE Antennas Wireless Propag. Lett.*, vol. 10, pp. 7–10, 2011.

[5] N. Nguyen-Trong, T. Kaufmann, L. Hall, and C. Fumeaux, "Optimization of leaky-wave antennas based on non-uniform HMSIW," in *Proc. IEEE MTT-S Int. Conf. Numer. Electromagn. Multiphys. Optim.*, Aug. 2015, pp. 1–4.

[6] W. Menzel, "A new travelling wave antenna in microstrip," in *Proc. 8th Eur. Microw. Conf.*, Sep. 1978, pp. 302–306.

[7] H. Ermert, "Guiding and radiation characteristics of planar waveguides," *IEE J. Microw. Opt. Acoust.*, vol. 3, no. 2, pp. 59–62, Mar. 1979.

[8] A. A. Oliner, "Leakage from higher modes on microstrip line with application to antennas," *Radio Sci.*, vol. 22, no. 6, pp. 907–912, 1987.

[9] D. K. Karmokar, K. P. Esselle, and S. G. Hay, "Fixed-frequency beam steering of microstrip leaky-wave antennas using binary switches," *IEEE Trans. Antennas Propag.*, vol. 64, no. 6, pp. 2146–2154, Jun. 2016.

[10] D. K. Karmokar, K. P. Esselle, and T. S. Bird, "An array of half-width microstrip leaky-wave antennas radiating on boresight," *IEEE Antennas Wireless Propag. Lett.*, vol. 14, pp. 112–114, 2015.

[11] G. M. Zelinski, G. A. Thiele, M. L. Hastriter, M. J. Havrilla, and A. J. Terzuoli, "Half width leaky wave antennas," *Microw., Antennas Propag.*, vol. 1, no. 2, pp. 341–348, Apr. 2007.

[12] C. Jin and A. Alphones, "Leaky-wave radiation behavior from a double periodic composite right/left-handed substrate integrated waveguide," *IEEE Trans. Antennas Propag.*, vol. 60, no. 4, pp. 1727–1735, Apr. 2012.

[13] J. Machac, M. Polivka, and K. Zemlyakov, "A dual band leaky wave antenna on a CRLH substrate integrated waveguide," *IEEE Trans. Antennas Propag.*, vol. 61, no. 7, pp. 3876–3879, Jul. 2013.

[14] S. S. Haghighi, A. A. Heidari, and M. Movahhedi, "A three-band substrate integrated waveguide leaky-wave antenna based on composite right/left-handed structure," *IEEE Trans. Antennas Propag.*, vol. 63, no. 10, pp. 4578–4582, Oct. 2015.

[15] "CST Microwave Studio," 2015. [Online]. Available: www.cst.com